Transmission Between Pairs of Hippocampal Slice Neurons: Quantal Levels, Oscillations, and LTP

ROBERTO MALINOW*

Long-term potentiation (LTP) of synaptic transmission after coincident pre- and postsynaptic activity is considered a cellular model of changes underlying learning and memory. In intact tissue, LTP has been observed only between populations of neurons, making analysis of mechanisms difficult. Transmission between individual pre- and postsynaptic hippocampal cells was studied, suggesting quantal amplitude distributions with little variability in quantal size. LTP between such pairs is manifested by large, persistent, and synapse-specific potentiation with a shift in amplitude distribution that suggests presynaptic changes. Oscillations in amplitude of transmission, apparently of presynaptic origin, are common and can be triggered by LTP.

THE INDUCTION OF LTP REQUIRES simultaneous activity within a population of input cells to activate postsynaptic *N*-methyl-D-aspartate (NMDA) receptors (*1*). However, it has generally been assumed that, once established, LTP is a property of individual synapses. This notion was challenged by a study suggesting that coactivity within a population of neurons is required for expression of LTP (*2*). I have now tested whether LTP can be expressed between individual CA3 and CA1 neurons with the use of whole-cell recording techniques (*3, 4*), methods that allow greater control of postsynaptic membrane potential and better signal resolution than do intracellular recordings.

I studied transmission between individual neurons in hippocampal slices by impaling a presynaptic CA3 neuron intracellularly and monitoring a postsynaptic CA1 neuron with a whole-cell pipette (Fig. 1A). Four such synaptically connected pairs were studied (*5*). Average synaptic currents were small (0.57 ± 0.2 pA, mean ± SEM), and the time course of the variance did not reveal an obvious synaptic event (Fig. 1B) (*6*). Amplitudes of presumptive synaptic events could be estimated by integration of the current over a fixed time window after the capacitative coupling artifact (*7*). From these measurements, density estimates of the amplitude distribution, made with the use of a Gaussian kernel (*8*), revealed events for which the amplitudes were outside the range of the noise (Fig. 1, D and E). There was a clear initial peak that matched the density estimate of the noise and was assumed to represent failures of transmission (*4*). Other peaks appeared distinct, with half-widths no greater than that of the noise (*9*) (Fig. 1, D and E). These results suggest that a quantal event with variance considerably less than that of the noise, which in this case is about the amplitude of a quantum, could be discerned (*10*).

Pairing presynaptic activity with postsynaptic depolarization for 40 stimuli induced a persistent potentiation of synaptic transmission (Figs. 1C and 2A). The time course of the variance now revealed a synaptic event with an amplitude that fluctuated more than the noise (Fig. 1C). This potentiation was associated with a marked change in the density estimate, which showed a large decline of failures and a shift in responses from a skewed distribution to a more symmetric pattern (Fig. 1F). In addition, quantal size appeared to have increased ~50%, an amount expected to make a small contribution to the 1000 to 2000% enhancement in transmission. The potentiation of transmission was persistent (Fig. 2A), lasting the 1.5 hours of the dual recording. Basal synaptic transmission, monitored through a separate pathway onto the same postsynaptic cell, remained relatively constant, demonstrating that the enhancement was restricted to transmission between the two coactivated neurons (Fig. 2B). The percent failure rate, estimated from the density distribution (*4, 8*), decreased immediately after pairing (Fig. 2C). These results were found in the four pairs of synaptically connected cells that demonstrated potentiated transmission after pairing (Fig. 3). These findings are consistent with those obtained in slices with the use of stimulation for which it was uncertain whether a single presynaptic cell was being activated (*4, 11*).

The decrease in failures and shift in the amplitude distribution with LTP could result from an increase in the probability that a given quantum of transmitter will be released, p, or from an increase in the number of releasable quanta, n. To determine whether changes occur in n or in p, one can estimate these values for epochs before and during LTP with various fitting algorithms (*12*). However, data obtained with pairs of cells or minimal stimulation (*13, 4*) generally showed oscillatory amplitudes of transmission with periods ranging from 2 to 15 min (Fig. 4). Thus, epochs with sufficient number of values to determine n and p showed nonstationarities, which preclude the use of standard fitting algorithms (*14*).

The basis of these oscillations was examined by computation of the inverse square of the coefficient of variance (CV^{-2}), which can be an indicator of presynaptic function (*4, 11, 15*). This statistic oscillated in phase

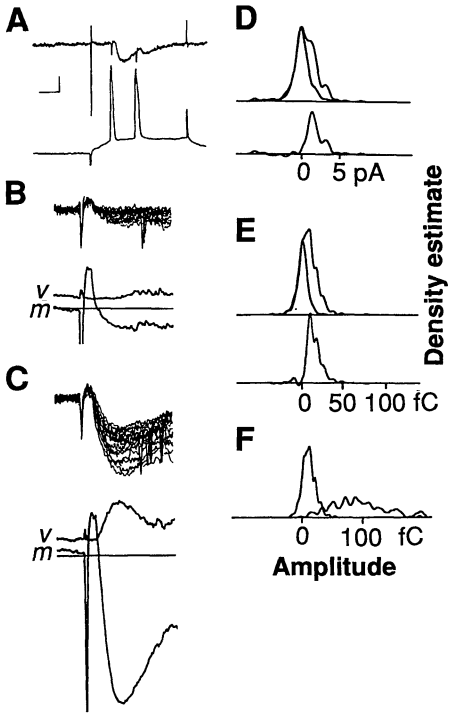

Fig. 1. Synaptic transmission between individual CA3 and CA1 neurons displays quantal transmission and LTP. (**A**) Simultaneous whole-cell recording from a postsynaptic CA1 neuron (top) and intracellular recording from a presynaptic CA3 neuron (bottom). (**B** and **C**) Ten consecutive synaptic currents before (B) and during (C) LTP, with time courses of m and the variance (v) about m of 220 sweeps. (**D**) Density estimates of the peak amplitude distribution (*8*) of 220 consecutive sweeps before LTP. EPSC amplitude is estimated by averaging over a fixed 2-ms window at the peak of response and subtracting this value from a fixed 2-ms window before response (*7*). Noise is estimated by placing the same windows at the baseline period. Top traces display density estimate of the noise (half-width, 1.4 pA) and EPSC amplitude. Lower trace is the digital subtraction of the noise peak from EPSC amplitude distribution, revealing the amplitude distribution of quantal events (half-width of first peak, 1.2 pA). (**E**) Density estimate using synaptic charge (integrated current over fixed 30-ms window). (**F**) Density estimates of the synaptic charge distribution of 220 consecutive sweeps before (left) and during (right) LTP. Transmission failures are nearly absent and there is a large shift in density estimate to a symmetric shape during LTP. Calibration bars: (A) 25 ms, 20 pA (top), 15 mV (bottom). (B) 10 ms, 4 pA (top), 2 pA (m). (C) 10 ms, 4 pA (top), 2 pA (m).

Department of Molecular and Cellular Physiology, Stanford University, Stanford, CA 94305, and Department of Physiology and Biophysics, University of Iowa, Iowa City, IA 52242.

*Present address: Department of Physiology and Biophysics, University of Iowa, Iowa City, IA 52242.

with the mean amplitude (m) (Fig. 4), suggesting that the oscillations were in presynaptic mechanisms. Furthermore, the oscillations were often more prominent in CV^{-2} than in the mean. If the release process is assumed to satisfy binomial statistics (at least for short epochs), then $m = npa$ and $CV^{-2} = np/(1 - p)$, where a is the quantal size. Therefore, oscillations in p (rather than in n or a) could explain this observation because changes in p would be expected to affect CV^{-2} more than they would affect m (*4, 15*). In 6 of 17 cases (including cell pairs and minimal stimulation) (Fig. 4B), these oscillations were absent before pairing and were triggered by the LTP-inducing pairing protocol (16). The remainder of cases appeared to show oscillations before and after pairing (17).

The synaptic currents recorded between individual central nervous system neurons were generally small, but quantal events with variance smaller than their amplitude were readily detected. This differs from the case for cultured neurons, in which synaptic currents are considerably larger and the variance of elemental events is large compared to the size of the event (*18*).

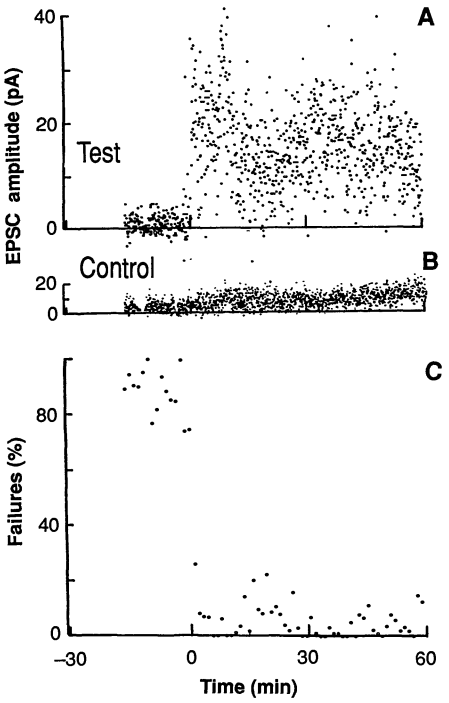

Fig. 2. LTP between individual CA3 and CA1 neurons is synapse-specific and associated with a rapid decrease in transmission failures. (**A**) Amplitude of EPSC in a CA1 cell, elicited every 4 s by generation of an action potential in a CA3 neuron. At time 0, the CA1 cell was depolarized until large slow spikes inactivated (*24*). At the cell body the voltage was about +10 mV. A presynaptic CA3 cell was repeatedly stimulated to generate action potentials by current pulse injection 40 times at 2 Hz. CA1 voltage was subsequently brought back to −65 mV and test stimuli were resumed. (**B**) Amplitude of EPSC in the same CA1 cell as in (A), elicited by stimulation of a separate group of axons with an extracellular stimulating electrode. (**C**) Percent synaptic failures for a 3-min window, plotted every 1 min.

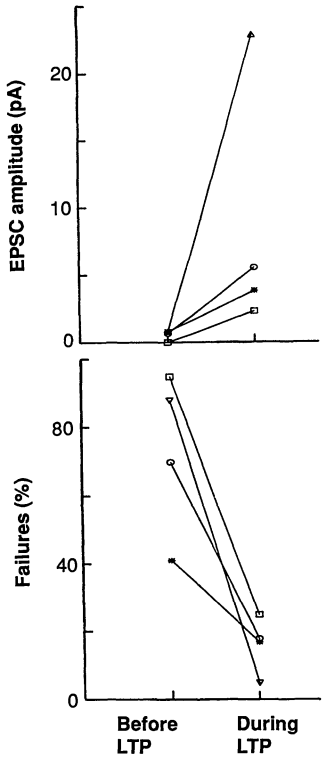

Fig. 3. The increase in mean EPSC amplitude is associated with a comparable decrease in transmission failure rate. (**Top**) Mean EPSC for four examples showing LTP with pairing. The EPSC amplitude increases from 0.57 ± 0.2 pA to 8.6 ± 5 pA. (**Bottom**) Corresponding decrease in transmission failure rate from 74 ± 14% to 16 ± 5%.

This study reports LTP between individual neurons in tissue slices, supporting the view that activity-induced changes in transmission can be localized to individual synapses (*19*). The enhancement observed in this study was large, persistent, and synapse-specific. The magnitude of potentiation could be more than tenfold, considerably larger than the magnitudes typically seen in population studies. Furthermore, a previous comprehensive study (*2*) consistently failed to see the expression of LTP between individual CA3 and CA1 neurons. These differential levels of potentiation may be explained by differences in the methods used for inducing LTP. In this study, with whole-cell access to the postsynaptic cell, the subsynaptic membrane potential may have been more depolarized than in cases where depolarization was provided by a tetanus. Tetanic stimulation may fully depolarize, and thereby fully potentiate, only a small subpopulation of electrically close synapses. A test synapse could easily fall outside this small subpopulation of synapses that show large potentiation. Alternatively, microelectrode recordings may bias the sample set to pairs of cells with large, and therefore already potentiated, levels of transmission.

After the induction of LTP, the synaptic responses displayed fewer failures of transmission and shifted from a skewed to a symmetric amplitude distribution, changes most easily explained by a presynaptic increase in the number of vesicles available for release or the probability that a vesicle will be released (*4, 11*). In addition, there was a small change in quantal size, allowing for some postsynaptic modification.

Oscillations in the size of the response were observed that appear to be of presynaptic origin and that can be triggered by LTP-inducing stimuli. These fluctuations resemble periodic release of quanta at the neuromuscular junction (*20*) that are hypothesized to result from oscillations in intracellular Ca^{2+} (*21*) at the prejunctional terminal; these oscillations, in turn, are

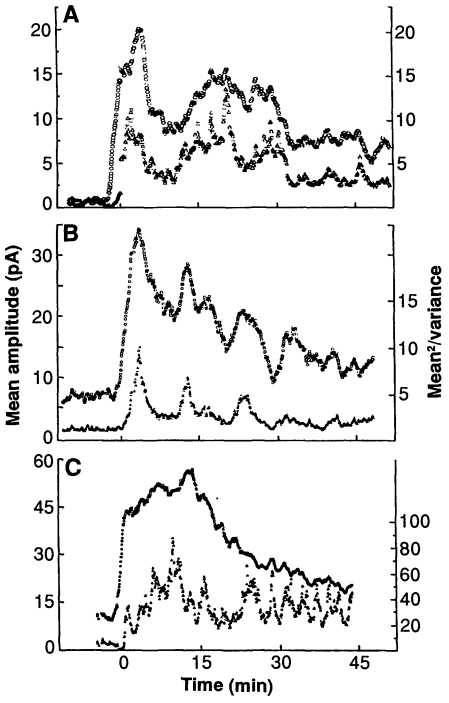

Fig. 4. Oscillations in the amplitude of transmission and presynaptic function. Time course of mean response and CV^{-2} for three experiments with (**A**) intracellular stimulation of presynaptic CA3 cell or (**B** and **C**) minimal stimulation. Each point in the graphs represents the mean (upper curve) or CV^{-2} (mean²/variance) (lower curve) (*4*) of a moving window of 50 (A and B) and 25 (C) values. Pairing of presynaptic activity with postsynaptic depolarization at time 0 as described for Fig. 2. Oscillations begin after the pairing protocol in B. The period of the oscillations was independent of the window size, but oscillation amplitudes and CV^{-2} values tended to diminish as the window size approached the size of the period. Consequently, oscillations of period less than ~2 min would not be detectable with this averaging method.

thought to affect the probability of quantum release (*22*). Because LTP is triggered postsynaptically (*23*), after its postsynaptic induction a retrograde messenger could be released, affecting presynaptic Ca^{2+} homeostasis and yielding Ca^{2+} oscillations and increased transmitter release. It is possible that different synaptic inputs active during the induction of LTP become associated by showing synchronized, oscillating potentiated transmission.

REFERENCES AND NOTES

1. T. Bliss and M. Lynch, in *Long-Term Potentiation: Mechanisms and Key Issues*, P. Landfield and S. Deadwyler, Eds. (Liss, New York, 1988); R. Nicoll, J. Kauer, R. Malenka, *Neuron* **1**, 97 (1988); T. Brown *et al.*, *Science* **242**, 724 (1988).
2. M. Friedlander, R. Sayer, S. Redman, *J Neurosci.* **10**, 814 (1990).
3. O. Hamill, A. Marty, E. Neher, B. Sakmann, F. Sigworth, *Pfluegers Arch.* **391**, 85 (1981); F. Edwards, A. Konnerth, B. Sakmann, T. Takahashi, *ibid.* **414**, 600 (1989); M. Blanton, J. Lo Turco, A. Kriegstein, *J Neurosci. Methods* **30**, 203 (1989).
4. R. Malinow and R. W. Tsien, *Nature* 346, 177 (1990).
5. Transverse hippocampal slices (400 to 500 μm) from 3- to 5-week-old rats [B. Alger and R. Nicoll, *J. Physiol. (London)* **328**, 105 (1982)] were submerged and superfused continuously with a modified Earle's solution [119 mM NaCl, 2.5 mM KCl, 1.3 mM $MgCl_2$, 2.5 mM $CaCl_2$, 1.0 mM NaH_2PO_4, 26.2 mM $NaHCO_3$, and 11 mM glucose, saturated with 95% O_2 plus 5% CO_2, pH 7.4 at 22°C]. Excitatory postsynaptic currents (EPSCs) were recorded with a patch electrode (3 to 7 megaohm tip resistance, no fire polishing or Sylgard coating) in the whole-cell mode (Axopatch 1D). Pipette solution contained 100 mM cesium gluconate, 0.6 mM EGTA, 5 mM $MgCl_2$, 2 mM adenosine triphosphate, 0.3 mM guanosine triphosphate, 40 mM Hepes, pH adjusted to 7.2 with CsOH. Holding potential was kept constant between −60 and −70 mV. EPSCs were amplified 50 to 500 times, filtered at 1 kHz, and digitized at 10 kHz. Recordings were obtained from six synaptically connected pairs of neurons, but only four showed LTP, and these were further analyzed. Approximately 50 pairs of cells were probed for synaptic connections.
6. These synaptic connections would not be detectable by intracellular recordings because this method has lower signal-to-noise resolution.
7. R. Sayer, S. Redman, P. Andersen, *J. Neurosci.* **9**, 840 (1989).
8. V. Silverman, *Density Estimate for Statistics and Data Analysis* (Chapman & Hall, New York, 1986).
9. Integration of the current over a larger fixed window (Fig. 1E) revealed more peaks than with a small window (Fig. 1D), possibly because of asynchronous elicited release of transmitter.
10. Because the recording noise variance and quantal variance are additive, finding a variance equal to that of the noise implies that there is negligible quantal variance relative to the noise, which, in this case, has a variance close to the quantal amplitude, ~1 to 2 pA. For comparison, see G. Hess and co-workers [*Neurosci. Lett.* 77, 187 (1987)] and R. Sayer and co-workers [*J. Neurosci.* **10**, 826 (1990)]. Estimates of the number of channels responsible for the quantum depend on cable filtering, single-channel conductance, and open times; none of these values is known for these synapses. The quantal bumps on the density estimate of the amplitude distribution appeared not to be an artifact of a small sample size because they appeared only to the right of the zero peak and because amplitude distributions generated with every other sweep were similar.
11. J. Bekkers and C. Stevens, *Nature* **346**, 724 (1990).
12. S. Redman, *Physiol. Rev.* **70**, 165 (1990).
13. B. McNaughton, C. Barnes, P. Andersen, *J. Neurophysiol.* **46**, 952 (1981).
14. T. Brown, D. Perkel, M. Feldman, *Proc. Natl. Acad. Sci.* **73**, 2913 (1976). These nonstationarities would tend to minimize the estimate of $m = np$, and may, in part, account for the lack of change in m with LTP noted by T. Foster and B. McNaughton [*Hippocampus* **1**, 79 (1991)] and the smaller changes in CV^{-2} than in the mean noted in (*4*).
15. J. del Castillo and B. Katz, *J. Physiol. (London)* **124**, 560 (1954).
16. This finding also argues against the possibility that the oscillations are an artifact resulting from sampling aliasing, which could cause apparent oscillations but would not be expected to change with the pairing protocol.
17. This may indicate that oscillations can be independent of LTP or that LTP induction before the recording session had induced oscillations.
18. J. Bekkers, G. Richerson, C. Stevens, *Proc. Natl. Acad. Sci. U.S.A.* **87**, 5359 (1990).
19. Estimates of synaptic connections between individual CA3 and CA1 neurons suggest a very low number of synapses [D. Amaral, N. Ishizuka, B. Claiborne, *Prog. Brain Res.* **83**, 1 (1990)].
20. H. Meiri and R. Rahamimoff, *J. Physiol. (London)* **278**, 513 (1978); P. Pawson and A. Grinnell, *Proc. R. Soc. London Ser. B* **237**, 489 (1989).
21. M. Berridge and A. Galione, *FASEB J.* **2**, 3074 (1988).
22. R. Zucker, *Annu. Rev. Neurosci.* **12**, 13 (1989).
23. H. Wigstrom, B. Gustafsson, Y.-Y. Huang, W. Abraham, *Acta Physiol. Scand.* **126**, 317 (1986); B. R. Sastry, J. W. Goh, A. Auyeung, *Science* **232**, 988 (1986); S. Kelso, A. Ganong, T. Brown, *Proc. Natl. Acad. Sci. U.S.A.* **83**, 5326 (1986); R. Malinow and J. Miller, *Nature* **320**, 529 (1986).
24. These are presumably action potentials mediated by Ca^{2+} channels thought to be located at dendrites [R. Westenbroek, M. Ahlijanian, W. Catterall, *Nature* **347**, 281 (1990)] and may be used as an indicator of dendritic depolarization.

25. I thank R. W. Tsien for support and discussions and A. Jones of Reed College for illuminating statistical help. Supported by University of Iowa College of Medicine Startup Grant to R.M. and a Javits Investigator Award to R.W.T.

10 December 1990; accepted 4 March 1991

Effect of Light Chain V Region Duplication on IgG Oligomerization and in Vivo Efficacy

WALTER SHUFORD, HOWARD V. RAFF, J. WILLIAM FINLEY, JAMES ESSELSTYN, LINDA J. HARRIS*

A human immunoglobulin G_1 (IgG_1) antibody oligomer was isolated from a transfected myeloma cell line that produced a monoclonal antibody to group B streptococci. Compared to the IgG_1 monomer, the oligomer was significantly more effective at protecting neonatal rats from infection in vivo. The oligomer was also shown to cross the placenta and to be stable in neonatal rats. Immunochemical analysis and complementary DNA sequencing showed that the transfected cell line produced two distinct kappa light chains: a normal light chain (L_n) with a molecular mass of 25 kilodaltons and a 37-kilodalton species (L_{37}), the domain composition of which was variable-variable-constant (V-V-C). Cotransfection of vectors encoding the heavy chain and L_{37} resulted in production of oligomeric IgG.

BOTH IMMUNOGLOBULIN M (IGM) and IgG antibodies can enhance phagocytic clearance of microbial pathogens. Each immunoglobulin class has unique properties, which if appropriately combined could result in an antibody with improved characteristics. Because of their pentameric structure, IgM antibodies can exhibit higher avidity binding to antigen than IgG antibodies with identical intrinsic affinities. Activation of complement component C1 requires multivalent binding of the C1q subunit of C1. Such binding can be provided by a single pentameric IgM molecule or at least two IgG molecules in close proximity (*1*). Therefore, on a per molecule basis, IgM antibodies are often more efficient opsonins. IgG antibodies, however, have the advantages of extended in vivo half-life and, because of their ability to interact with Fc receptors, cross the placenta and contribute to neonatal immunoprophylaxis (*2*). A human IgM monoclonal antibody (MAb) was developed as a potential immunotherapeutic agent for neonatal bacterial sepsis caused by group B streptococci (GBS) (*3*). To compare the in vitro and in vivo activities of IgG_1 and IgM forms of this antibody, we used recombinant DNA techniques to produce both antibody classes. During the production of the IgG_1 antibodies, an oligomeric IgG was formed that appears to have combined some of the desirable characteristics of both IgM and IgG antibodies. We now compare the molecular composition and functional properties of the oligomeric and monomeric IgG antibodies.

The vector pNkA1.1 consists of a complete kappa (κ) light (L) chain gene derived

W. Shuford, H. V. Raff, J. Esselstyn, Department of Immune Sciences, Bristol-Myers Squibb Pharmaceutical Research Institute–Seattle, Seattle, WA 98121. J. W. Finley and L. J. Harris, Department of Molecular Immunology, Bristol-Myers Squibb Pharmaceutical Research Institute–Seattle, Seattle, WA 98121.

*To whom correspondence should be addressed.